

Causal Effect Estimation with Learned Instrument Representations

Frances Dean ^{*1 2} Jenna Fields ^{*1 2} Radhika Bhalerao ^{1 2} Marie Charpignon ¹ Ahmed Alaa ^{1 2}

Abstract

Instrumental variable (IV) methods mitigate bias from unobserved confounding in observational causal inference but rely on the availability of a valid instrument, which can often be difficult or infeasible to identify in practice. In this paper, we propose a representation learning approach that constructs *instrumental representations* from observed covariates, which enable IV-based estimation even in the absence of an explicit instrument. Our model (ZNet) achieves this through an architecture that mirrors the structural causal model of IVs; it decomposes the ambient feature space into confounding and instrumental components, and is trained by enforcing *empirical moment conditions* corresponding to the defining properties of valid instruments (i.e., relevance, exclusion restriction, and instrumental unconfoundedness). Importantly, ZNet is compatible with a wide range of downstream two-stage IV estimators of causal effects. Our experiments demonstrate that ZNet can (i) recover ground-truth instruments when they already exist in the ambient feature space and (ii) construct latent instruments in the embedding space when no explicit IVs are available. This suggests that ZNet can be used as a “plug-and-play” module for causal inference in general observational settings, regardless of whether the (untestable) assumption of unconfoundedness is satisfied.

1. Introduction

Instrumental variable (IV) regression is a commonly used approach to address unobserved confounding when estimating causal effects from observational data. An IV randomizes the treatment without having a direct effect on the outcome, enabling estimation of causal effects with two stage regression (Imbens & Rubin, 2015). For example, in economics,

¹University of California, Berkeley ²University of California, San Francisco. Correspondence to: Frances Dean <frances_dean@berkeley.edu>, Jenna Fields <jenna_fields@berkeley.edu>.

Preprint. February 12, 2026.

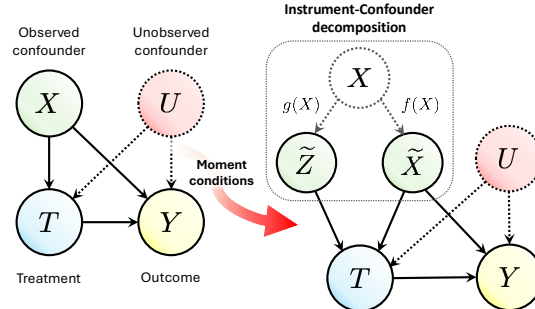


Figure 1. Causal inference with learned instruments. We learn a feature representation of the observed data X that decomposes them into a learned instrument $\tilde{Z} = g(X)$ and a residual confounder $\tilde{X} = f(X)$. This decomposition is induced by enforcing the moment conditions needed for the learned instrument \tilde{Z} to be valid.

geographical proximity to a college is used as an instrument for educational attainment in estimating the returns of schooling (Card, 1993) and draft lotteries as instruments to study the effect of military service on long-term economic outcomes (Angrist, 1990). In medicine, genetic variants have been used as IVs since they often highly correlate with risk factors but do not directly influence the outcomes associated with these factors (Davey Smith & Hemani, 2014). While IV regression enables causal identification in observational data, these methods are not ubiquitous because a suitable instrument must be available and known to the analyst. This is seldom the case in many applications. For instance, in health research, genetic variants are rarely available in large datasets, and moreover, candidate genes may not be strong or valid IVs (Davies et al., 2015; Burgess et al., 2016).

The tradition of IV regression originated in settings with tabular data, where an instrument is expected to be explicitly observed within the feature space. In contrast, the increasing use of deep learning representations of high-dimensional data, such as text, images, and multimodal inputs, creates new opportunities to uncover instrumental variables that are implicit rather than directly observed. For example, medical images may encode subtle provider- or institution-specific patterns, while rich electronic health records may imitate genetic or phenotypic information through descriptions embedded in clinical notes. Representation learning methods could be used to extract such latent variables as instruments, thereby automating instrument selection and further extend-

ing IV methods to non-tabular settings where no single variable in the ambient feature space is a valid IV on its own.

In this paper, we develop a representation learning approach that constructs IVs from observed data by decomposing the input feature space into confounding and instrumental components (Fig. 1). Our model, which we call ZNet, is an encoder architecture that mirrors the *structural causal model* (SCM) of IVs and is regularized by enforcing the *empirical moment conditions* that correspond to the defining properties of valid instruments (i.e., relevance, exclusion restriction, and instrumental unconfoundedness). The learned instrumental representation can then be used as input to standard two-stage IV estimators to recover causal effects. When a valid IV is present in the ambient feature space, ZNet recovers a representation that is strongly correlated with it; when no explicit instrument exists, ZNet learns a latent representation that can serve as a pragmatic instrument. The ZNet architecture is compatible with a broad class of downstream IV estimators, and through semi-synthetic experiments we show that learning instrumental representations substantially reduces bias from unobserved confounding. Additionally, we illustrate the learned feature decomposition in real-world, high-dimensional settings using electrocardiogram data.

2. Preliminaries

Let $Y \in \mathcal{Y} \subset \mathbb{R}$ denote a continuous outcome, $T \in \mathcal{T} \subset \mathbb{R}$ a treatment variable, and $X \in \mathcal{X} \subset \mathbb{R}^d$ a set of observed covariates associated with each unit. The treatment T has a causal effect on the outcome Y , while X may influence both T and Y (X confounds the relation of primary interest between T and Y). In addition to the measured confounders X , there are unknown or *unobserved confounders* U , which induce spurious associations by simultaneously affecting both the treatment and outcome (Fig. 1). We assume that the outcome variable Y is determined by the following SCM:

$$Y = \varphi(X, T) + e_Y(U), \quad T = \psi(X) + e_T(U), \quad (1)$$

for unknown functions $\varphi : \mathcal{X} \times \mathcal{T} \rightarrow \mathcal{Y}$ and $\psi : \mathcal{X} \rightarrow \mathcal{T}$. Following (Hartford et al., 2017), we assume that the unobserved confounders U influence the outcome Y and the treatment T additively, via the error functions of U , which we henceforth denote e_Y and e_T . As a result, the observational and interventional distributions generally differ, i.e.,

$$\begin{aligned} \mathbb{E}[Y|X, T] &= \varphi(X, T) + \mathbb{E}[e_Y|X, T] \\ &\neq \varphi(X, T) + \mathbb{E}[e_Y|X] = \mathbb{E}[Y|do(T), X]. \end{aligned}$$

Thus, standard regression would lead to confounding bias.

De-confounding with instrumental variables (IVs). A common method for removing confounding bias is to use IV regression. In the classical IV setting, we assume access to an additional variable Z that is not influenced by the unobserved confounders U , affects the treatment T , and has no

direct effect on the outcome Y (Verbeek, 2004; Angrist et al., 1996). Formally, given a set of observed confounders X, Z is a valid IV if it satisfies the following conditions:

$$\begin{aligned} \text{Relevance: } Z &\not\perp T | X, \\ \text{Exclusion restriction: } Z &\perp Y | (X, T, U), \\ \text{Unconfoundedness: } Z &\perp U | X. \end{aligned} \quad (2)$$

Under these conditions, the instrument Z can be used in a two-stage regression to estimate the effect of T on Y . Under the additive model in (1), Hartford et al. (2017) uses the instrument Z to set up an inverse problem by relating the counterfactual $\mathbb{E}[Y|do(T), X]$ to observable distributions:

$$\begin{aligned} \mathbb{E}[Y|X, Z] &= \mathbb{E}[\varphi(X, T) + e_Y|X, Z] \\ &= \mathbb{E}[\varphi(X, T)|X, Z] + \mathbb{E}[e_Y|X] \\ &= \int \mathbb{E}[Y|do(T), X] dF(T|X, Z). \end{aligned} \quad (3)$$

Thus, with the instrument Z , we can estimate the counterfactual $\mathbb{E}[Y|do(T), X]$ by estimating the two observable functions $\mathbb{E}[Y|X, Z]$ and $F(T|X, Z)$. While this inverse problem is ill-posed, it provides a practical framework for estimating counterfactuals, and identification is possible under certain conditions (Newey & Powell, 2003).¹ A two-stage regression fits a model $\hat{F}(T|X, Z)$, and estimates $\mathbb{E}[Y|do(T), X]$ by replacing $F(T|X, Z)$ with $\hat{F}(T|X, Z)$ in (3). With an estimate of $\mathbb{E}[Y|do(T), X]$, we can derive the conditional average treatment effects (CATE) and average treatment effects (ATE):

$$\begin{aligned} \text{CATE}(X) &= \mathbb{E}[Y|do(T) = 1, X] - \mathbb{E}[Y|do(T) = 0, X], \\ \text{ATE} &= \mathbb{E}[Y|do(T) = 1] - \mathbb{E}[Y|do(T) = 0]. \end{aligned} \quad (4)$$

Equation (3) is notably more general than IV regression with linear models. We allow $\mathbb{E}[e_Y|X] \neq 0$, i.e., observed confounders can correlate with unobserved errors. In two stage least square regression (TSLS), confounders cannot be endogenous for unbiased estimates (Verbeek, 2004).

3. Learning Instruments from Data

In the absence of a (known) valid instrument Z , our method learns an instrumental representation directly from the features X using an observational dataset $\{(X_i, T_i, Y_i)\}_i$.

Instrument-confounder decompositions. As illustrated in Fig. 1, we seek a pair of functions $(f(\cdot), g(\cdot))$ that decompose the observed features \tilde{X} into an observed *confounding* component C and an *instrumental* component \tilde{Z} , i.e.,

$$(\tilde{X}, \tilde{Z}) = (f(X), g(X)), \quad (5)$$

¹For example, in the linear case, Two-Stage Least Squares Regression (TSLS) allows for identification of causal effects.

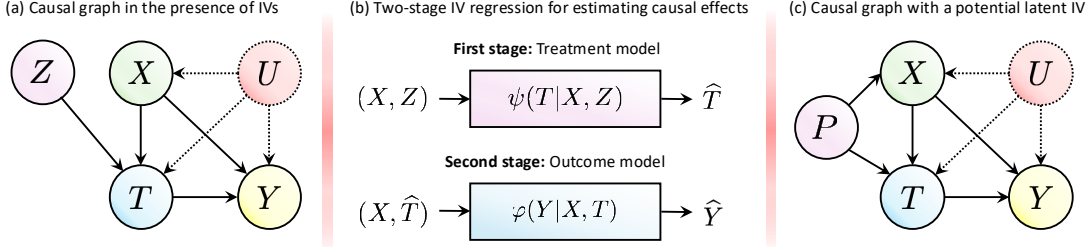


Figure 2. **Illustration of the IV setting.** (a) Causal graph for the IV setting; (b) When an IV exists, causal effects can be estimated under unobserved confounding by first fitting a model ψ to predict T from (X, Z) , and then training a model φ that predicts outcomes based on predicted treatments. (c) Illustration for the latent instrument example discussed in Section 3. Here, P is the provider identity.

such that $g(X)$ satisfies the three IV conditions in (2), and the function $f(X)$ fits the additive SCM in (1), i.e.,

$$Y = \varphi(f(X), T) + e_Y(U), \quad T = \psi(f(X)) + e_T(U).$$

Notice that this construction is broadly applicable and captures many real-world scenarios for how instrumental variations may be encoded in the feature space. First, consider the scenario where a subset of the observed variables can already serve as a valid instrument, i.e., $Z \subset X$. In this setting, the decomposition trivially reduces to $g(X) = Z$ and $f(X) = X \setminus Z$. Second, consider scenarios in which the instrument is latent but can be inferred from proxy signals in the observed features X . For example, in healthcare settings, providers are often quasi-randomly assigned and have different propensities to administer treatments based on their interpretation of patient information, while provider identity itself does not directly affect outcomes. Although provider identifiers may not be explicitly recorded, their influence shows in retrospective data through visit timing, laboratory and diagnostic tests ordered, and clinical notes (Fig. 2(c)). A representation of provider influence can therefore be learned from X via $g(\cdot)$ and used as an instrumental variable.

While the instrument–confounder decomposition is motivated by real-world scenarios, our model does not require an *a posteriori* interpretation of the learned instrument \tilde{Z} . Satisfaction of the three IV conditions allows for a pragmatic implementation of IV regression independent of interpretation, since our decomposition treats instruments as abstract mathematical constructs in a latent embedding space, even when no explicitly identifiable instrumental variable exists. Consequently, our method can be applied without prior domain knowledge on the existence of valid instruments.

Moment conditions on $f(\cdot)$ and $g(\cdot)$. A valid decomposition of the observed features X into confounding and instrumental components must induce a factorization of the joint distribution $\mathbb{P}(g(X), f(X), U, T, Y)$ that is consistent with the SCM defined by (1) and (2). In particular, the relevance condition requires that the instrumental component $g(X)$ be predictive of the treatment, i.e., $\text{Cov}(g(X), T) \neq 0$. Exclu-

sion restriction requires that all direct effects of X on the outcome Y be mediated through the confounding component $\tilde{X} = f(X)$; equivalently, $\text{Cov}(f(X), Y) \neq 0$ while $\text{Cov}(f(X), g(X)) = 0$. As we discuss later in detail in Section 5, we enforce these covariance relationships through the architecture and loss function of our proposed model.

The covariance structure described above ensures that the learned instrument \tilde{Z} will be unconfounded and independent of the error e_Y as long as X is unconfounded by U . The assumption that X is not influenced by U is standard to allow for classical IV regression and straightforward IV generation (Yuan et al., 2022; Li & Yao, 2024; Cheng et al., 2023; Chou et al., 2024). Since our feature decomposition produces both a confounder and an instrument, we add an additional constraint based on the following Lemma to ensure that \tilde{Z} is valid even when X may be influenced by U .

Lemma 1. *If $Z \sim \mathcal{N}(0, \sigma^2)$, and suppose that the random variables (Z, e_Y, X, T) satisfy $\text{Cov}(Z, e_Y - \mathbb{E}[e_Y|X, T]) = 0$. Then it follows that $\text{Cov}(Z, e_Y) = 0$.*

Proof. Notice that as $\mathbb{E}[Z] = 0$, we have

$$\begin{aligned} 0 &= \text{Cov}(Z, e_Y - \mathbb{E}[e_Y|X, T]) \\ &= \mathbb{E}[Z(e_Y - \mathbb{E}[e_Y|X, T])] - \mathbb{E}[Z] \mathbb{E}[(e_Y - \mathbb{E}[e_Y|X, T])] \\ &= \mathbb{E}[Z(e_Y - \mathbb{E}[e_Y|X, T])] \\ &= \mathbb{E}[Z \cdot e_Y] - \mathbb{E}[Z] \mathbb{E}[e_Y|X, T] = \text{Cov}(Z, e_Y). \quad \square \end{aligned}$$

This additional covariance term can be evaluated by fitting a regression model for $\hat{Y} = \mathbb{E}[Y|X, T]$ and then computing its residuals as $Y - \mathbb{E}[Y|X, T]$. Notice that $Y - \mathbb{E}[Y|X, T] = Y - \varphi(X, T) - (E[Y|X, T] - \varphi(X, T)) = e_Y - \mathbb{E}[e_Y|X, T]$. Regardless of whether any existing instruments are normally distributed, if we can construct $g(X) = \tilde{Z} \sim \mathcal{N}(0, \sigma^2)$ to have no covariance with the residuals $e_Y - \mathbb{E}[e_Y|X, T]$, i.e. with $\tilde{\varepsilon}_Y := Y - \mathbb{E}[Y|X, T]$, then \tilde{Z} has zero covariance with e_Y by Lemma 1. To sum up, f and g need to satisfy the following moment restrictions:

Moment Condition 1: $\text{Cov}(g(X), \tilde{\varepsilon}_Y) = 0$.

Moment Condition 2: $\text{Cov}(g(X), f(X)) = 0$.

Moment Condition 3: $\text{Cov}(f(X), Y) > 0$.

Moment Condition 4: $\text{Cov}(T, g(X)) > 0$.

4. Related Work

Prior work on learning IVs has largely focused on the problem of IV selection from a set of observed candidates. For instance, ModeIV chooses instruments by looking at clusters of treatment effects based on weighting the observed variables used as instruments (Hartford et al., 2021). DIV-VAE uses a variational autoencoder (VAE) approach to disentangle an instrumental variable under the assumption that a surrogate instrument exists in the data (Cheng et al., 2024). IV-Tetrad (Silva & Shimizu, 2017) builds strong instruments requiring at least two observed IV candidates. Several methods for refining IV candidates and estimating causal effects from these candidates can fall under this category as well, including the sisVIVE (Kang et al., 2016), TEDVAE (Zhang et al., 2021) and Ivy models (Kuang et al., 2020) among various others (Davies et al., 2015; Burgess et al., 2016).

Methods to learn IVs were also proposed in prior work, including GIV (Wu et al., 2023), AutoIV (Yuan et al., 2022), VIV (Li & Yao, 2024), DVAE-CIV (Cheng et al., 2023), and GDIV (Chou et al., 2024). GIV generates a categorical IV with unsupervised expectation-maximization that groups data according to underlying distributional differences assumed to arise from the aggregation of data from multiple sources. This approach uses environment as an IV in data coming multiple sources (Schweisthal et al., 2024). The other methods learn variational distributions. The AutoIV method uses a mutual information (MI) based loss to generate an abstract IV from observed data by learning variational distributions (Yuan et al., 2022). VIV, DVAE-CIV, and GDIV use VAEs to learn independent latent variables that serve as Z, U, C from the observed data Y, T, X , sometimes including an additional adjustment variable A derived from Y, X . VAEs have shown great success in probabilistic modeling in general but lack theory to guarantee learning the true causal model and satisfaction of IV conditions.

5. The ZNet Model

5.1. ZNet Architecture

The ZNet architecture encodes an inductive prior consistent with the SCM of the IV setup in (1). The ZNet model comprises two encoders, f and g , which learn representations of the confounders \tilde{X} and the instrument \tilde{Z} , respectively, along with three feedforward neural networks, Φ, φ and π , used to estimate $\mathbb{E}[Y|X, T]$, $\mathbb{E}[Y|\tilde{X}, T]$ and $\mathbb{E}[T|\tilde{Z}]$. An overview of all components of the ZNet model is shown in Fig. 3. After training, ZNet produces embeddings $\{\tilde{X}, \tilde{Z}\}$ from the observed features X , which we then use to transform the ob-

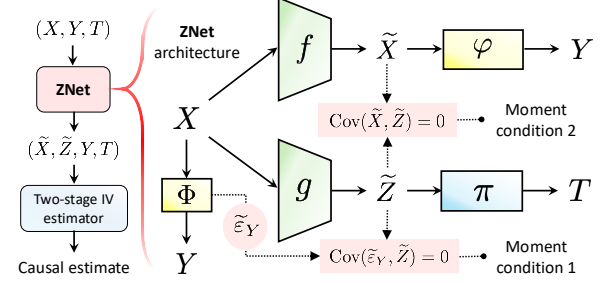


Figure 3. Overview of the components of the ZNet Architecture.

servational dataset $\mathcal{D} = \{(X_i, T_i, Y_i)\}_i$ into a new dataset $\tilde{\mathcal{D}} = \{(\tilde{X}_i, \tilde{Z}_i, T_i, Y_i)\}_i$ with the learned instruments $\{\tilde{Z}_i\}_i$. Importantly, as we show in the experiments section, ZNet is compatible with any downstream IV-based causal estimator.

5.2. ZNet Loss Function

We first train the network Φ to obtain the regression residual $\tilde{\varepsilon}_Y = Y - \mathbb{E}[Y|X, T]$, and then train the ZNet model end by minimizing the predictive loss of the supervised learning models φ and π , and imposing the moment conditions on the learned embeddings (\tilde{X}, \tilde{Z}) as discussed in Section 3, i.e.,

$$\min_{f, g, \varphi, \pi} \mathcal{L}_Y(\varphi(f)) + \mathcal{L}_T(\pi(g)) \text{ s.t. } \begin{cases} \text{Cov}(g(X), \tilde{\varepsilon}_Y) = 0, \\ \text{Cov}(f(X), g(X)) = 0. \end{cases}$$

Here, $\mathcal{L}_Y(\varphi(f))$ and $\mathcal{L}_T(\pi(g))$ are supervised losses for the models $\varphi(f(X), T)$ and $\pi(g(X))$ against the labels Y and T (e.g., mean squared error and cross entropy losses). Note that moment conditions 3 and 4 in Section 3 are implicit in these losses. We train ZNet through a Lagrangian relaxation of the constrained optimization problem above as follows:

$$\begin{aligned} \min_{f, g, \varphi, \pi} & \mathcal{L}_Y(\varphi(f)) + \mathcal{L}_T(\pi(g)) + \lambda_0 \text{Cov}(g(X), \tilde{\varepsilon}_Y) \\ & + \lambda_1 \text{Cov}(f(X), g(X)), \end{aligned}$$

where λ_0 and λ_1 are tunable hyperparameters. Our training algorithm approximates the covariance terms above using a weighted combination of Pearson correlation coefficients or mutual information, as described in the next section.

5.3. ZNet Implementation and Training Details

The networks Φ, φ, π, f, g are implemented as feedforward networks, where the activation function can be chosen between ReLU or linear. Supervised learning losses for Φ, φ and π are implemented as mean squared error (MSE), MSE, and binary cross entropy (BCE), respectively.

Empirical approximation of moment constraints. The covariance terms in the ZNet loss function are approximated through either the squared Pearson correlation or an approximation of the mutual information (MI) using kernel density

estimation (KDE) with Gaussian kernels; the selection of the approximation method is treated as a hyperparameter. We augment the standard supervised losses for φ, π with the option of learning these networks through moment constraints as well. In this case, each network’s loss is implemented as the complement of Pearson or MI correlation. To encourage the distribution of the resulting instrumental variable \tilde{Z} to follow a normal distribution following Lemma 1, we add distribution restrictions using a Kullback-Leibler (KL) divergence penalty on each dimension of \tilde{X} and \tilde{Z} with a standard normal distribution \mathcal{N} . We also constrain the average correlation across dimensions within \tilde{X} and \tilde{Z} to encourage the features of the learned representations to be distinct. The overall loss with approximate $\widehat{\text{Cov}}(\cdot)$ is thus given as:

$$\begin{aligned}\mathcal{L}_{\text{ZNet}} = & \alpha_1 \text{MSE}(\varphi(f(X), T), Y) \\ & + \alpha_2 \text{BCE}(\pi(g(X)), T) \\ & + \alpha_3 (1 - \widehat{\text{Cov}}(\varphi(f(X), T), Y))^2 \\ & + \alpha_4 (1 - \widehat{\text{Cov}}(\pi(g(X)), T))^2 \\ & + \alpha_5 \widehat{\text{Cov}}(g(X), \tilde{\varepsilon}_Y)^2 + \alpha_6 \widehat{\text{Cov}}(\pi(g(X)), T)^2 \\ & + \alpha_7 \text{KL}(g(X), \mathcal{N}) + \alpha_8 \text{KL}(f(X), \mathcal{N}) \\ & + \alpha_9 \widehat{\text{Cov}}(g(X))^2 + \alpha_{10} \widehat{\text{Cov}}(f(X))^2 \\ & + \alpha_{11} \text{MSE}(\Phi(f(X)), Y).\end{aligned}$$

Training steps. ZNet training occurs in three stages. First, the network Φ is separately trained to estimate $\tilde{\varepsilon}_Y$, i.e. only α_{11} is non-zero. Weights of Φ are then frozen. Next the full network is pretrained by fitting φ, π in a supervised setting without the moment constraints ($\alpha_5 = \alpha_6 = \alpha_7 = \alpha_8 = \alpha_9 = \alpha_{10} = \alpha_{11} = 0$). This serves to encourage starting representations of \tilde{X} and \tilde{Z} to be highly correlated with Y and T , respectively. Finally, the full ZNet model is finetuned end-to-end across all the loss terms above (with $\alpha_{11} = 0$).

Hyperparameter tuning. All hyperparameters, including all loss term weights and whether the moment constraints are approximated via Pearson correlations or MI, were tuned using Bayesian optimization implemented in Botorch (Balandat et al., 2020). We perform optimization corresponding to the two stages of IV regression. For each IV generation, we maximize the instrument’s relevance F-Statistic and minimize the correlation between learned \tilde{X} and \tilde{Z} using Botorch’s native adaptation of the Noisy Expected Improvement acquisition function for multi-objective optimization. We then choose the parameter set from the Pareto front with the highest F-Statistic. We tune the treatment effect estimators to simultaneously minimize the MSE of the model’s ATE against a nearest-neighbors (NN) ATE and the MSE of estimated factual Y , again with the Noisy Expected Improvement acquisition function. The parameter set is selected from the Pareto front by the least MSE of NN.

5.4. Causal Effect Estimation

Recall that ZNet creates a dataset with learned confounders and instruments, and is therefore compatible with a wide range of downstream IV-based estimators of causal effects. We wrap our ZNet model around three downstream estimators of treatment effects to demonstrate the utility of ZNet in causal inference: TSLS, DFIV and DeepIV. Each method takes as input the true treatment term T and our learned representations \tilde{X} and \tilde{Z} . TSLS is the classical IV estimator. It assumes linear structural equations and independence of U and X , thus we omit when not applicable (Imbens & Rubin, 2015; Verbeek, 2004). DeepIV (Hartford et al., 2017) generalizes TSLS by allowing the model at each stage to be parameterized by a neural network and $X \not\perp U$. The DFIV estimator allows basis functions at each stage to be parametrized by neural networks (Xu et al., 2020).

6. Experiments

Datasets. We conduct a comprehensive and extensive evaluation experiments of ZNet using the semi-synthetic **IHDP** dataset, a widely used benchmark for causal inference (Hill, 2011). IHDP is based on an experiment that studied the effect of home visits during infancy on cognitive test scores of premature infants, with 985 individuals and 25 covariates. We design multiple experimental setups using IHDP that correspond to different ways in which IVs may explicitly or implicitly exist. Each setup is defined by three sets of features, $X^{\rightarrow T}$, $X^{\rightarrow Y}$, and $X^{\leftarrow U}$, where we each $X^{\rightarrow I}$ is the subset of covariates X which have causal influence on I in the arrow’s direction. We create four experimental setups based on their inclusion of an instrument:

- **Disjoint Candidate:** $\exists X^{\rightarrow T}$ s.t. $X^{\rightarrow T} \cap X^{\rightarrow Y} = \emptyset, X^{\rightarrow T} \cap X^{\leftarrow U} = \emptyset$.
- **Mixed Candidate:** $\exists \tilde{X}^{\rightarrow T} \subset X^{\rightarrow T}$ s.t. $\tilde{X}^{\rightarrow T} \cap X^{\rightarrow Y} = \emptyset, \tilde{X}^{\rightarrow T} \cap X^{\leftarrow U} = \emptyset$.
- **Latent Categorical Instrument:** $\exists Z, f$ s.t. $f(X^{\rightarrow T}) = Z \in \mathbb{N}^+$.
- **No Candidate:** $\nexists \tilde{X}^{\rightarrow T} \subseteq X^{\rightarrow T}$ s.t. $\tilde{X}^{\rightarrow T} \cap X^{\rightarrow Y} = \emptyset, \tilde{X}^{\rightarrow T} \cap X^{\leftarrow U} = \emptyset$.

Directed acyclic graphs for all settings above are included in the Appendix. For each setting, we consider scenarios where $X^{\leftarrow U} \neq \emptyset$ and $X^{\leftarrow U} = \emptyset$. We also consider data where $U = \emptyset$ (i.e. no unobserved confounding). After fixing a covariate set, we choose functions ϕ, ψ, e_Y, e_T and generate

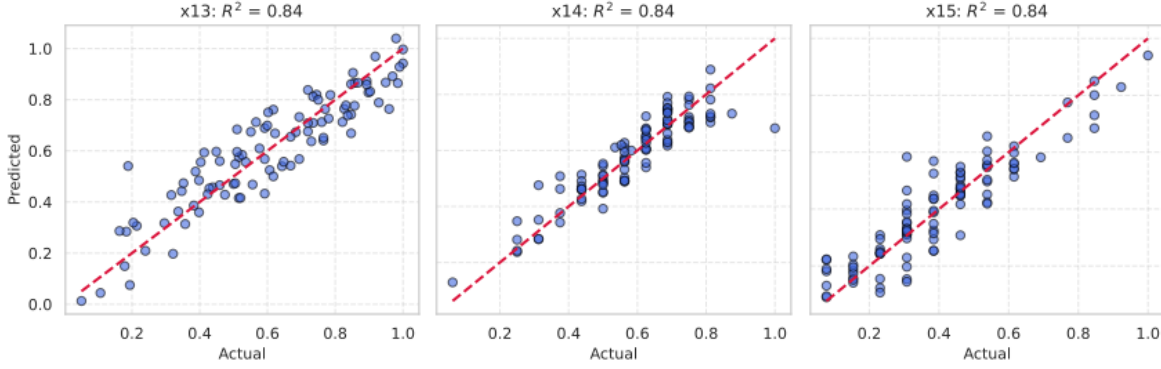


Figure 4. Regression plots for learned and true instruments. Learned instruments are correlated to true ones in the setup with true instrument candidate. Here, X_{13}, X_{14}, X_{15} are true IVs (x -axis) plotted against the corresponding dimensions of the learned \tilde{Z} (y -axis).

the variables Y, T similar to (Wu et al., 2023) by writing

$$Y = \phi(X_Y, T) + e_Y(U) + \varepsilon_Y \text{ for } \varepsilon_Y \sim \mathcal{N}(0, .1),$$

$$T \sim \text{Bernoulli}(P) \text{ for } P = \psi(X_T) + e_T(U) + \varepsilon_T,$$

for $\varepsilon_T \sim \mathcal{N}(0, .1)$. We focus on binary treatments, though ZNet is easily adapted for continuous settings. We consider linear and non-linear version of ϕ, ψ for each dataset. For each scenario, we randomly generate 10 datasets with varying functions $\phi, e_Y, \varepsilon_Y, \psi, e_T, \varepsilon_T$. Across dataset and confounding settings, this means we evaluate ZNet on a comprehensive collection of 180 datasets. Data are always split into 60% for training, 20% for tuning, and 20% for testing. All experiments report results on the test proportion.

Metrics and baselines. All model performances were evaluated using bootstrapping ($N=50$). ATE errors are evaluated in terms of absolute proportions: $|\text{Estimate} - \text{True}|/|\text{True}|$. Error on CATE estimation is presented as average square error in estimated individual level effect (PEHE). In addition to prior methods discussed in Section 4, we compare ZNet-learned instruments to using the true instrument *TrueIV*, if it exists, and to TARNET (Shalit et al., 2017), a CATE estimation model used in the absence of unobserved confounding.

Table 1. Evaluating the average instrumental properties of ZNet learned representations

Metric	ZNet (Train / Val / Test)	TrueIV (Train / Val / Test)
F-Stat(\tilde{Z}, T)	140.25 / 14.82 / 8.70	57.36 / 19.35 / 8.18
Corr(\tilde{Z}, \tilde{X})	0.15 / 0.16 / 0.19	0.09 / 0.10 / 0.16
Corr(\tilde{Z}, U)	0.13 / 0.13 / 0.15	0.03 / 0.06 / 0.06
Corr(\tilde{Z}, ε_Y)	0.02 / 0.06 / 0.09	0.04 / 0.05 / 0.08

6.1. ZNet Instrument Representations

As shown in Fig. 4, ZNet successfully recovers existing instruments. In the **Linear Mixed Candidate** setting, there

Table 2. Mean absolute ATE proportional error (SE) across all experimental settings with the DeepIV and DF-IV estimators.

Downstream	Model	Datasets	$ \text{ATE} $ Error
	TARNET	180	0.442 (0.03)
	TrueIV	120	0.406 (0.03)
DeepIV	ZNet	180	0.412 (0.03)
	AutoIV		0.440 (0.03)
	VIV		0.438 (0.04)
	GIV		0.429 (0.03)
DF IV	TrueIV	120	0.604 (0.09)
	ZNet	180	0.544 (0.04)
	AutoIV		0.705 (0.06)
	VIV		0.652 (0.11)
	GIV		0.798 (0.07)

are three variables $X_{13}, X_{14}, X_{15} \in X^{\rightarrow T}$ which are explicit instruments. In one selected sample dataset, ZNet generates a 10-dimensional variable Z which is correlated with and linearly predicts each of X_{13}, X_{14}, X_{15} . ZNet also recovers latent instruments. Consider an example **Linear Categorical Instrument** dataset. The true instrument groups the observed data into 5 clusters. ZNet approximately recovers these clusters by regression, using t-SNE dimensionality reduction, and K-Means with cluster relabeling in Fig. 5.

Independent of the existence of an instrument in the observed data, the ZNet model generates a representation that is correlated with T , independent of the confounder representation \tilde{X} , independent of the error in predicting Y , and unconfounded by U . We evaluate the suitability of these instrument representations empirically. We observe F-Statistics that indicate the predictive power of generated representations \tilde{Z} for T and low correlation across prohibited relationships between \tilde{Z} and confounders. ZNet IV condition satisfaction is strong on average over all 180 datasets compared to the average over existing dataset IVs

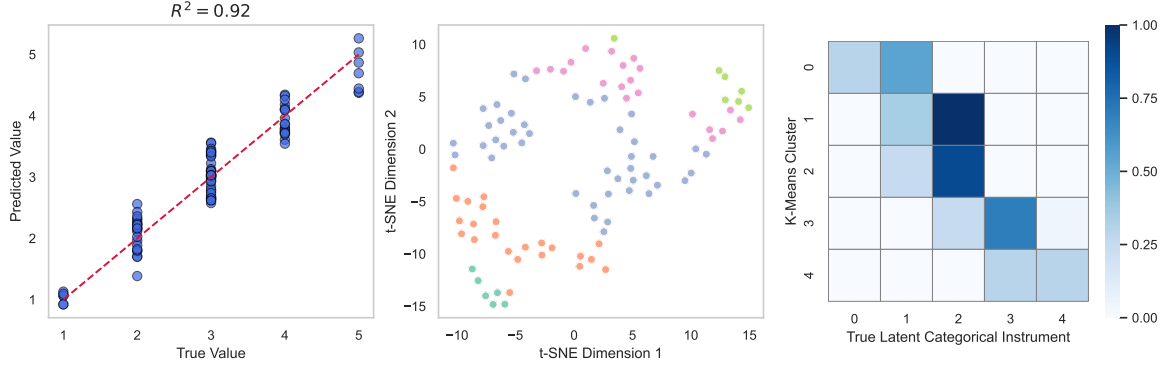


Figure 5. Learned instrument representations are correlated to existing instruments in latent categorical instrument dataset. Left most plot are regression predictions of the true categorical IV using learned \tilde{Z} . Middle plot is a t-SNE visualization of \tilde{Z} colored by the true IV. Right most is a normalized confusion matrix of K-means clusters of \tilde{Z} compared to the true instruments.

(Table 1). We additionally compare satisfaction by dataset scenarios in Appendix Tables 11, 12.

6.2. Causal Effect Estimation with ZNet

We used the ZNet learned instrument representations to recover the causal effects using a second stage regression with DeepIV or DFIV. We assess performance across the all experimental settings. We highlight performance across three comparisons: (1) all 180 datasets, (2) the 80 datasets with confounding influencing X , i.e. $U \rightarrow X$ datasets, and (3) the 40 confounded datasets with no instrument candidate.

The first comparison shows that the performance of ZNet in estimating ATE outperforms baselines across the different experimental settings (Table 2). Notably, ZNet is the only method that outperforms TARNet, which ignores unobserved confounding altogether. Additionally, ZNet performs best in the setting where the unobserved confounding influences the observed data, i.e. $U \rightarrow X$ datasets (Table 3). This is because our loss construction guarantees this owing to the inclusion of the first moment condition (Lemma 1).

Table 3. Mean absolute ATE proportional error (SE) across $U \rightarrow X$ datasets with the DeepIV and DF-IV estimators.

Downstream	Model	Datasets	$ \text{ATE} $ Error
	TARNet	80	0.666 (0.06)
DeepIV	TrueIV	60	0.534 (0.05)
	ZNet		0.620 (0.06)
	AutoIV	80	0.677 (0.06)
	VIV		0.702 (0.07)
DF IV	GIV		0.672 (0.06)
	TrueIV	60	0.736 (0.17)
	ZNet		0.729 (0.08)
	AutoIV	80	0.870 (0.10)
	VIV		0.906 (0.15)
	GIV		0.860 (0.09)

The performance comparison in Table 4 focuses on the most common setting where explicit instrument candidates are not available. ZNet once again outperforms existing IV generation methods and TARNet. Performance on causal effect estimation was worse using DF IV than DeepIV consistently regardless of data generation method. We also include additional results stratified by the data generation settings which show where IV estimation is easier or more challenging and results of analyses with TSLS in the appendix (See Appendix Tables 7, 8). We report results on the PEHE in CATE estimation, which similarly varies by data generation settings, in the appendix as well (Appendix Tables 9, 10).

Table 4. Mean absolute ATE proportional error (SE) across confounded settings with no true instrument candidate.

Downstream	Model	Datasets	$ \text{ATE} $ Error
	TARNet	40	0.619 (0.10)
DeepIV	ZNet		0.566 (0.09)
	AutoIV	40	0.667 (0.10)
	VIV		0.654 (0.11)
	GIV		0.704 (0.11)
DF IV	ZNet		0.773 (0.14)
	AutoIV	40	0.837 (0.14)
	VIV		0.986 (0.28)
	GIV		1.077 (0.17)

6.3. Application of ZNet to Unstructured Data

ZNet in the unstructured data setting is particularly powerful because high dimensional data can contain additional information recoverable as an instrument more readily. We believe this is especially impactful in the setting of unstructured health data. We demonstrate the ability of ZNet to recover instruments in such settings using a semi-synthetic electrocardiogram (ECG) dataset. Data from 35,463 ECGs from a public Physionet dataset serve as X , age and sex

serve as hidden confounders U , and variables T and Y are sampled, analogous to the process for IHDP data, in this case as a random linear combination of eight interpretable, derived features of the ECG, i.e. heart rate, QT interval, QRS amplitude, etc. (Zheng et al., 2022; 2000; Goldberger et al., 2000 (June 13)). As with most unstructured health data, no true instrument exists. Despite that, ZNet still recovers an instrument representation and more accurately predicts treatment effects than ordinary least squares regression using the tabular features (Table 5). Here, we use ZNet with Deep IV since it is consistently more accurate than DF-IV.

Table 5. Mean absolute ATE proportional error (SE) across bootstraps in the ECG dataset.

Downstream	Model	ATE Error
DeepIV	ZNet	0.126 (0.000647)
	OLS	0.665 (0.00263)

These ECG data come from two hospitals in Zhejiang, China. In true observational data, both treatments received and images taken can vary by care setting due to purchased equipment or physician propensity despite being random with respect to many confounders. Moreover, the outcomes associated to treatments are typically uncorrelated with hospital setting directly. While hospital setting is not available in the ECG data and its instrumental value hidden to an analyst, with ZNet, we extract a representation that satisfies instrument properties potentially leveraging this latent information as illustrated pictorially in Fig. 6. We evaluate the instrument selected by ZNet by its satisfaction of IV properties as correlations in Table 6. Values suggest a relevant instrument that through weak correlations in prohibited relations also satisfies exclusion restriction and unconfoundedness.

Table 6. Evaluating the IV conditions of the ECG based instrument.

Metric	ZNet ECG IV (Train / Val / Test)
F-Stat(\tilde{Z}, T)	261.26 / 59.69 / 22.57
Cor(\tilde{Z}, \tilde{X})	0.0069 / 0.0064 / 0.0076
Cor(\tilde{Z}, U_1)	0.25 / 0.25 / 0.244
Cor(\tilde{Z}, U_2)	-0.15 / -0.16 / -0.15
Cor($\tilde{Z}, \tilde{\epsilon}_Y$)	0.0022 / 0.0048 / 0.015

7. Discussion

ZNet enables IV regression without domain knowledge of pre-existing IVs. This automation of IV generation from observed data is exciting, as it can enable the widespread use of IV regression for causal effect estimation. To this end, we contribute a comprehensive evaluation of IV generation for causal inference, which demonstrates broad utility. Regardless of the existence of a candidate or a latent instrument or of unobserved confounding, ZNet can exceed the

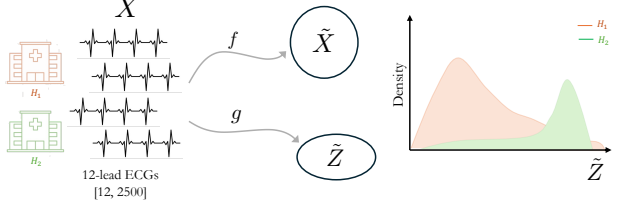


Figure 6. Visualization of ZNet with unstructured health data.

performance of TARNet and of probabilistic IV generation methods. This performance is enabled by the recovery of valid instrument representations. In the case of existing instruments among the observed data, we see that recovered instruments are highly correlated with these variables. Without candidates, ZNet representations are still relevant and show minimal correlation with hidden confounders and directly with the outcome.

The data generation process of any real world dataset is untestable. We can never confirm a lack of unobserved confounding, even when evaluating a candidate instrument. ZNet’s strong performance across settings suggests that it can serve as a “plug-in” causal inference estimator for causal inference in general observational settings, regardless of whether the untestable assumption of unconfoundedness is satisfied. Our evaluations show ZNet to be particularly well suited when unobserved confounders influence the observed data and where instrument candidates do not exist. These are the most challenging and general settings.

ZNet is especially relevant in the context of high dimensional unstructured data. Unstructured data may contain latent or abstract instruments more frequently, as high-dimensional feature spaces often contain rich information that our approach could learn to extract as instruments. High dimensional tabular and image data are becoming ubiquitous in the predictive models used across industries. Interest grows in embedding causal relationships into these models so that insights from their features are actionable. ZNet automatically mitigates unobserved confounding broadening the ability to pursue causal machine learning in predictive settings. We illustrate ZNet’s treatment effect estimation capability with ECGs, but applications for ZNet extend far beyond this modality and beyond healthcare.

Solutions to the ZNet loss minimization problem always give a representation that serves empirically as an instrument since empirical IV constraints are explicitly embedded in the loss function. This instrument can then be used in any downstream IV regression where satisfying the standard IV criteria (or, equivalently, ZNet moment constraints) implies the validity of subsequent causal inference. The strength and validity of ZNet generated instruments vary in finite settings. Variance in finite samples affects our ability to predict

treatment effects. However, IV estimation is also limited in general by a lack of theoretical guarantees of identifiability without conditions on the SCM. This theoretically limits not only our approach but IV estimation in general. Still, strong empirical results and opportunities in high dimensional data suggest the value in the increased use of these methods beyond linear settings.

Code

All code for running ZNet is available at <https://github.com/AlaaLab/ZNet.git>.

References

Angrist, J. D. Lifetime earnings and the vietnam era draft lottery: Evidence from social security administrative records. *American Economic Review*, 80(3):313–336, 1990.

Angrist, J. D., Imbens, G. W., and Rubin, D. B. Identification of causal effects using instrumental variables. *Journal of the American Statistical Association*, 91(434): 444–455, 1996. ISSN 01621459.

Balandat, M., Karrer, B., Jiang, D. R., Daulton, S., Letham, B., Wilson, A. G., and Bakshy, E. BoTorch: A Framework for Efficient Monte-Carlo Bayesian Optimization. In *Advances in Neural Information Processing Systems 33*, 2020.

Burgess, S., Dudbridge, F., and Thompson, S. G. Combining information on multiple instrumental variables in mendelian randomization: comparison of allele score and summarized data methods. *Statistics in medicine*, 35(11): 1880–1906, 2016.

Card, D. Using geographic variation in college proximity to estimate the return to schooling, 1993.

Cheng, D., Xu, Z., Li, J., Liu, L., Le, T. D., and Liu, J. Learning conditional instrumental variable representation for causal effect estimation. In *Joint European Conference on Machine Learning and Knowledge Discovery in Databases*, pp. 525–540. Springer, 2023.

Cheng, D., Li, J., Liu, L., Xu, Z., Zhang, W., Liu, J., and Le, T. D. Disentangled representation learning for causal inference with instruments. *IEEE Transactions on Neural Networks and Learning Systems*, 2024.

Chou, J., Chen, J., and Marathe, M. Estimate causal effects of entangled treatment on graphs using disentangled instrumental variables. In *2024 IEEE International Conference on Big Data (BigData)*, pp. 1260–1267. IEEE, 2024.

Davey Smith, G. and Hemani, G. Mendelian randomization: genetic anchors for causal inference in epidemiological studies. *Human molecular genetics*, 23(R1):R89–R98, 2014.

Davies, N. M., von Hinke Kessler Scholder, S., Farbmacher, H., Burgess, S., Windmeijer, F., and Smith, G. D. The many weak instruments problem and mendelian randomization. *Statistics in medicine*, 34(3):454–468, 2015.

Goldberger, A. L., Amaral, L. A. N., Glass, L., Hausdorff, J. M., Ivanov, P. C., Mark, R. G., Mietus, J. E., Moody, G. B., Peng, C.-K., and Stanley, H. E. PhysioBank, PhysioToolkit, and PhysioNet: Components of a new research resource for complex physiologic signals. *Circulation*, 101(23):e215–e220, 2000 (June 13).

Hartford, J., Lewis, G., Leyton-Brown, K., and Taddy, M. Deep iv: A flexible approach for counterfactual prediction. In *International Conference on Machine Learning*, pp. 1414–1423. PMLR, 2017.

Hartford, J. S., Veitch, V., Sridhar, D., and Leyton-Brown, K. Valid causal inference with (some) invalid instruments. In *International Conference on Machine Learning*, pp. 4096–4106. PMLR, 2021.

Hill, J. L. Bayesian nonparametric modeling for causal inference. *Journal of Computational and Graphical Statistics*, 20(1):217–240, 2011.

Imbens, G. W. and Rubin, D. B. *Causal Inference for Statistics, Social, and Biomedical Sciences: An Introduction*. Cambridge University Press, 2015.

Kang, H., Zhang, A., Cai, T. T., and Small, D. S. Instrumental variables estimation with some invalid instruments and its application to mendelian randomization. *Journal of the American statistical Association*, 111(513):132–144, 2016.

Kuang, Z., Sala, F., Sohoni, N., Wu, S., Córdova-Palomera, A., Dunnmon, J., Priest, J., and Re, C. Ivy: Instrumental variable synthesis for causal inference. In Chiappa, S. and Calandra, R. (eds.), *Proceedings of the Twenty Third International Conference on Artificial Intelligence and Statistics*, volume 108 of *Proceedings of Machine Learning Research*, pp. 398–410. PMLR, 26–28 Aug 2020.

Li, X. and Yao, L. Distribution-conditioned adversarial variational autoencoder for valid instrumental variable generation. In *Proceedings of the AAAI Conference on Artificial Intelligence*, volume 38, pp. 13664–13672, 2024.

Newey, W. K. and Powell, J. L. Instrumental variable estimation of nonparametric models. *Econometrica*, 71(5): 1565–1578, 2003.

Schweisthal, J., Frauen, D., Van Der Schaar, M., and Feuerriegel, S. Meta-learners for partially-identified treatment effects across multiple environments. In Salakhutdinov, R., Kolter, Z., Heller, K., Weller, A., Oliver, N., Scarlett, J., and Berkenkamp, F. (eds.), *Proceedings of the 41st International Conference on Machine Learning*, volume 235 of *Proceedings of Machine Learning Research*, pp. 43967–43985. PMLR, 21–27 Jul 2024.

Shalit, U., Johansson, F. D., and Sontag, D. Estimating individual treatment effect: generalization bounds and algorithms, 2017.

Silva, R. and Shimizu, S. Learning instrumental variables with structural and non-gaussianity assumptions. *Journal of Machine Learning Research*, 18(120):1–49, 2017.

Verbeek, M. *A Guide to Modern Econometrics*. John Wiley and Sons Ltd, 2004.

Wu, A., Kuang, K., Xiong, R., Zhu, M., Liu, Y., Li, B., Liu, F., Wang, Z., and Wu, F. Learning instrumental variable from data fusion for treatment effect estimation. In *Proceedings of the AAAI Conference on Artificial Intelligence*, volume 37, pp. 10324–10332, 2023.

Xu, L., Chen, Y., Srinivasan, S., de Freitas, N., Doucet, A., and Gretton, A. Learning deep features in instrumental variable regression. *arXiv preprint arXiv:2010.07154*, 2020.

Yuan, J., Wu, A., Kuang, K., Li, B., Wu, R., Wu, F., and Lin, L. Auto iv: Counterfactual prediction via automatic instrumental variable decomposition. *ACM Trans. Knowl. Discov. Data*, 16(4), January 2022. ISSN 1556-4681. doi: 10.1145/3494568.

Zhang, W., Liu, L., and Li, J. Treatment effect estimation with disentangled latent factors. In *Proceedings of the AAAI Conference on Artificial Intelligence*, volume 35, pp. 10923–10930, 2021.

Zheng, J., Chu, H., Struppa, D., Zhang, J., Yacoub, S. M., El-Askary, H., Chang, A., Ehwerhemuepha, L., Abu-dayyeh, I., Barrett, A., Fu, G., Yao, H., Li, D., Guo, H., and Rakovski, C. Optimal multi-stage arrhythmia classification approach. *Scientific Reports*, 10(2898), 2000.

Zheng, J., Guo, H., and Chu, H. A large scale 12-lead electrocardiogram database for arrhythmia study (version 1.0.0). *PhysioNet*, 2022.

A. Additional Figures

Table 7. ATE Results on Synthetic Linear Datasets

Dataset	Diff Means	TARNet	TSLS	IV Method	DeepIV	DF IV
Linear Disjoint	0.318	0.140	0.210	TrueIV	0.112	0.175
				ZNet	0.110	0.229
				AutoIV	<i>0.090</i>	0.329
				VIV	0.088	<i>0.184</i>
				GIV	0.113	0.537
Linear Disjoint (no $U \rightarrow X$)	0.267	0.207	0.327	TrueIV	0.148	0.280
				ZNet	0.222	0.469
				AutoIV	0.199	0.775
				VIV	0.190	0.269
				GIV	0.168	0.521
Linear Latent Categorical	0.160	0.157	1.118	TrueIV	0.101	<i>0.171</i>
				ZNet	0.090	0.080
				AutoIV	0.134	0.626
				VIV	0.092	0.353
				GIV	0.095	0.492
Linear Latent Categorical (no $U \rightarrow X$)	0.390	0.372	1.088	TrueIV	0.389	0.384
				ZNet	0.324	0.453
				AutoIV	0.343	0.723
				VIV	<i>0.309</i>	<i>0.411</i>
				GIV	0.298	0.535
Linear Mixed	0.790	0.570	0.448	TrueIV	<i>0.660</i>	0.592
				ZNet	0.537	0.844
				AutoIV	0.690	0.886
				VIV	0.716	0.859
				GIV	0.685	0.750
Linear Mixed (no $U \rightarrow X$)	0.390	0.298	0.326	TrueIV	0.314	0.446
				ZNet	<i>0.314</i>	0.535
				AutoIV	0.344	0.463
				VIV	<i>0.375</i>	<i>0.411</i>
				GIV	0.370	0.324
Linear No Candidate	1.749	1.375	-	TrueIV	-	-
				ZNet	1.306	1.724
				AutoIV	<i>1.418</i>	1.630
				VIV	1.460	1.429
				GIV	1.491	1.546
Linear No Candidate (no $U \rightarrow X$)	0.291	0.365	-	TrueIV	-	-
				ZNet	0.361	0.713
				AutoIV	0.405	0.831
				VIV	<i>0.367</i>	0.499
				GIV	0.435	1.193
Linear No Candidate (no U)	0.060	0.092	-	TrueIV	-	-
				ZNet	0.037	0.245
				AutoIV	0.064	0.823
				VIV	<i>0.043</i>	0.190
				GIV	0.052	0.556

Table 8. ATE Results on Synthetic Non-Linear Datasets

Dataset	Diff Means	TARNet	TSLS	IV Method	DeepIV	DF IV
Non-linear Disjoint	0.845	0.571	0.424	TrueIV	0.586	0.602
				ZNet	0.553	0.706
				AutoIV	0.656	0.869
				VIV	0.633	0.558
				GIV	0.551	0.854
Non-linear Disjoint (no $U \rightarrow X$)	0.172	0.255	0.349	TrueIV	0.202	0.661
				ZNet	0.274	0.354
				AutoIV	0.283	0.606
				VIV	0.218	0.339
				GIV	0.215	1.951
Non-linear Latent Categorical	1.441	0.784	12.998	TrueIV	0.697	1.758
				ZNet	0.689	0.784
				AutoIV	0.581	1.080
				VIV	0.798	0.678
				GIV	0.647	0.727
Non-linear Latent Categorical (no $U \rightarrow X$)	0.431	0.405	1.569	TrueIV	0.375	0.499
				ZNet	0.350	0.283
				AutoIV	0.376	0.319
				VIV	0.331	0.253
				GIV	0.299	0.810
Non-linear Mixed	1.501	1.190	1.570	TrueIV	1.051	1.118
				ZNet	1.200	1.005
				AutoIV	1.156	0.971
				VIV	1.179	1.397
				GIV	1.098	0.938
Non-linear Mixed (no $U \rightarrow X$)	0.205	0.342	0.535	TrueIV	0.232	0.564
				ZNet	0.379	0.327
				AutoIV	0.250	0.351
				VIV	0.245	1.786
				GIV	0.254	0.635
Non-linear No Candidate	0.658	0.542	–	TrueIV	–	–
				ZNet	0.478	0.457
				AutoIV	0.690	0.567
				VIV	0.654	1.788
				GIV	0.698	1.040
Non-linear No Candidate (no $U \rightarrow X$)	0.216	0.193	–	TrueIV	–	–
				ZNet	0.121	0.200
				AutoIV	0.155	0.321
				VIV	0.133	0.229
				GIV	0.190	0.528
Non-linear No Candidate (no U)	0.109	0.105	–	TrueIV	–	–
				ZNet	0.064	0.387
				AutoIV	0.079	0.513
				VIV	0.046	0.110
				GIV	0.068	0.433

Table 9. PEHE on Linear Synthetic Dataset.

Dataset	TARNet	IV Method	DeepIV	DF IV
Linear Disjoint	0.142	TrueIV	0.165	0.187
		ZNet	0.189	0.240
		AutoIV	0.150	0.323
		VIV	0.153	0.209
		GIV	0.188	0.445
Linear Disjoint (no $U \rightarrow X$)	0.176	TrueIV	0.202	0.272
		ZNet	0.203	0.431
		AutoIV	0.224	0.541
		VIV	0.215	0.273
		GIV	0.237	0.428
Linear Latent Categorical	0.213	TrueIV	0.264	0.259
		ZNet	0.239	0.212
		AutoIV	0.283	0.692
		VIV	0.263	0.470
		GIV	0.230	0.627
Linear Latent Categorical (no $U \rightarrow X$)	0.421	TrueIV	0.524	0.409
		ZNet	0.477	0.502
		AutoIV	0.508	0.676
		VIV	0.495	0.451
		GIV	0.471	0.501
Linear Mixed	0.681	TrueIV	0.805	0.800
		ZNet	0.692	1.167
		AutoIV	0.828	0.943
		VIV	0.836	0.969
		GIV	0.824	0.855
Linear Mixed (no $U \rightarrow X$)	0.385	TrueIV	0.527	0.672
		ZNet	0.593	0.817
		AutoIV	0.566	0.658
		VIV	0.599	0.536
		GIV	0.540	0.493
Linear No Candidate	0.726	TrueIV	—	—
		ZNet	0.741	0.935
		AutoIV	0.799	0.793
		VIV	0.825	0.777
		GIV	0.799	0.801
Linear No Candidate (no $U \rightarrow X$)	0.428	TrueIV	—	—
		ZNet	0.464	0.912
		AutoIV	0.563	0.884
		VIV	0.530	0.587
		GIV	0.568	1.321
Linear No Candidate (no U)	0.178	TrueIV	—	—
		ZNet	0.229	0.570
		AutoIV	0.342	1.553
		VIV	0.224	0.452
		GIV	0.313	0.932

Table 10. PEHE on Non-linear Synthetic Dataset.

Dataset	TARNet	IV Method	DeepIV	DF IV
Non-linear Disjoint	0.788	TrueIV	0.762	0.942
		ZNet	0.733	0.855
		AutoIV	0.805	1.028
		VIV	0.818	0.700
		GIV	0.753	0.930
Non-linear Disjoint (no $U \rightarrow X$)	0.548	TrueIV	0.509	0.834
		ZNet	0.528	1.253
		AutoIV	0.556	0.846
		VIV	0.523	0.567
		GIV	0.509	2.245
Non-linear Latent Categorical	0.529	TrueIV	0.561	1.121
		ZNet	0.515	0.548
		AutoIV	<i>0.519</i>	0.954
		VIV	0.626	0.552
		GIV	0.524	0.520
Non-linear Latent Categorical (no $U \rightarrow X$)	0.430	TrueIV	0.493	0.472
		ZNet	0.436	0.304
		AutoIV	0.527	0.397
		VIV	0.455	0.303
		GIV	0.446	0.709
Non-linear Mixed	0.965	TrueIV	0.818	0.786
		ZNet	0.988	0.866
		AutoIV	0.956	0.777
		VIV	1.005	0.882
		GIV	0.887	0.704
Non-linear Mixed (no $U \rightarrow X$)	0.952	TrueIV	0.842	0.963
		ZNet	0.854	0.859
		AutoIV	<i>0.841</i>	0.846
		VIV	0.858	2.192
		GIV	0.820	1.245
Non-linear No Candidate	0.648	TrueIV	–	–
		ZNet	0.624	0.615
		AutoIV	0.730	0.622
		VIV	0.724	1.417
		GIV	0.709	0.822
Non-linear No Candidate (no $U \rightarrow X$)	0.833	TrueIV	–	–
		ZNet	0.818	0.802
		AutoIV	0.820	<i>0.801</i>
		VIV	<i>0.805</i>	0.775
		GIV	0.793	1.249
Non-linear No Candidate (no U)	1.165	TrueIV	–	–
		ZNet	1.081	1.393
		AutoIV	1.158	1.415
		VIV	1.181	1.070
		GIV	<i>1.144</i>	<i>1.146</i>

Table 11. Instrument Strength and Validity Linear Synthetic Dataset.

Dataset	IV Method	F-Stat(Z,T) (Relevance) (Train/Val/Test)	Corr(Z,C) (Independence) (Train/Val/Test)	Corr(Z,Y-Yhat) (Exogeneity) (Train/Val/Test)	Corr(Z,U) (Independence) (Train/Val/Test)
Linear Disjoint	TrueIV	9.792 / 3.215 / 3.657	0.027 / 0.051 / 0.124	0.032 / 0.069 / 0.095	0.030 / 0.062 / 0.045
	ZNet	28.439 / 2.444 / 3.085	0.128 / 0.141 / 0.180	0.033 / 0.068 / 0.090	0.158 / 0.166 / 0.170
	AutoIV	5.275 / 1.880 / 2.731	0.208 / 0.221 / 0.243	0.000 / 0.000 / 0.000	0.104 / 0.109 / 0.098
	VIV	17.719 / 5.397 / 4.568	0.032 / 0.057 / 0.112	0.032 / 0.049 / 0.101	0.036 / 0.050 / 0.075
	GIV	8.737 / 2.217 / 3.190	0.139 / 0.143 / 0.173	0.032 / 0.039 / 0.067	0.080 / 0.084 / 0.111
Linear Disjoint (no $U \rightarrow X$)	TrueIV	17.167 / 7.477 / 6.471	0.027 / 0.051 / 0.124	0.051 / 0.056 / 0.116	0.035 / 0.049 / 0.095
	ZNet	45.214 / 8.188 / 3.851	0.080 / 0.111 / 0.149	0.025 / 0.052 / 0.095	0.029 / 0.056 / 0.093
	AutoIV	9.318 / 2.783 / 2.159	0.212 / 0.222 / 0.255	0.000 / 0.000 / 0.000	0.030 / 0.062 / 0.091
	VIV	16.739 / 3.926 / 3.641	0.030 / 0.058 / 0.119	0.025 / 0.065 / 0.109	0.036 / 0.053 / 0.080
	GIV	9.913 / 1.251 / 2.414	0.148 / 0.149 / 0.190	0.024 / 0.045 / 0.072	0.039 / 0.062 / 0.087
Linear Latent Categorical	TrueIV	165.204 / 53.555 / 19.690	0.202 / 0.206 / 0.230	0.011 / 0.014 / 0.028	0.035 / 0.048 / 0.076
	ZNet	179.695 / 25.554 / 9.951	0.134 / 0.134 / 0.165	0.014 / 0.039 / 0.071	0.074 / 0.081 / 0.098
	AutoIV	68.529 / 18.436 / 6.537	0.258 / 0.247 / 0.263	0.000 / 0.000 / 0.000	0.144 / 0.154 / 0.156
	VIV	17.504 / 5.266 / 5.422	0.035 / 0.064 / 0.118	0.030 / 0.039 / 0.097	0.036 / 0.056 / 0.082
	GIV	97.670 / 25.682 / 12.462	0.140 / 0.157 / 0.178	0.020 / 0.024 / 0.065	0.036 / 0.067 / 0.081
Linear Latent Categorical (no $U \rightarrow X$)	TrueIV	199.602 / 65.321 / 24.395	0.204 / 0.212 / 0.235	0.006 / 0.016 / 0.031	0.036 / 0.049 / 0.065
	ZNet	300.974 / 25.263 / 11.940	0.111 / 0.117 / 0.138	0.010 / 0.053 / 0.085	0.043 / 0.058 / 0.073
	AutoIV	91.941 / 28.877 / 8.274	0.249 / 0.263 / 0.266	0.000 / 0.000 / 0.000	0.031 / 0.054 / 0.074
	VIV	16.884 / 4.987 / 4.814	0.034 / 0.058 / 0.115	0.024 / 0.042 / 0.099	0.031 / 0.064 / 0.081
	GIV	35.204 / 24.341 / 9.507	0.146 / 0.146 / 0.191	0.017 / 0.038 / 0.056	0.029 / 0.054 / 0.082
Linear Mixed	TrueIV	8.070 / 2.816 / 3.181	0.027 / 0.051 / 0.124	0.081 / 0.099 / 0.113	0.030 / 0.062 / 0.045
	ZNet	221.401 / 25.663 / 20.673	0.209 / 0.208 / 0.238	0.013 / 0.053 / 0.084	0.284 / 0.240 / 0.303
	AutoIV	103.603 / 22.816 / 23.096	0.209 / 0.211 / 0.235	0.000 / 0.000 / 0.000	0.253 / 0.219 / 0.289
	VIV	18.179 / 5.523 / 4.300	0.033 / 0.053 / 0.111	0.030 / 0.044 / 0.112	0.050 / 0.072 / 0.091
	GIV	43.053 / 8.902 / 8.220	0.147 / 0.150 / 0.195	0.026 / 0.041 / 0.080	0.124 / 0.117 / 0.157
Linear Mixed (no $U \rightarrow X$)	TrueIV	12.066 / 5.101 / 3.489	0.027 / 0.051 / 0.124	0.063 / 0.081 / 0.097	0.027 / 0.060 / 0.079
	ZNet	133.538 / 16.742 / 8.084	0.150 / 0.155 / 0.186	0.025 / 0.077 / 0.114	0.045 / 0.055 / 0.094
	AutoIV	104.522 / 31.072 / 17.727	0.237 / 0.241 / 0.261	0.000 / 0.000 / 0.000	0.029 / 0.049 / 0.094
	VIV	16.356 / 7.037 / 3.971	0.033 / 0.060 / 0.117	0.028 / 0.053 / 0.101	0.042 / 0.055 / 0.086
	GIV	12.316 / 2.874 / 4.237	0.150 / 0.159 / 0.194	0.027 / 0.026 / 0.063	0.029 / 0.042 / 0.095
Linear No Candidate	TrueIV	—	—	—	—
	ZNet	141.454 / 17.320 / 8.324	0.150 / 0.168 / 0.199	0.019 / 0.070 / 0.079	0.327 / 0.310 / 0.295
	AutoIV	88.696 / 23.879 / 11.640	0.245 / 0.240 / 0.272	0.000 / 0.000 / 0.000	0.404 / 0.399 / 0.373
	VIV	18.248 / 4.797 / 4.426	0.033 / 0.059 / 0.115	0.039 / 0.062 / 0.098	0.057 / 0.074 / 0.098
	GIV	52.157 / 15.182 / 5.950	0.145 / 0.141 / 0.186	0.029 / 0.039 / 0.075	0.124 / 0.144 / 0.134
Linear No Candidate (no $U \rightarrow X$)	TrueIV	—	—	—	—
	ZNet	71.331 / 2.770 / 3.064	0.166 / 0.181 / 0.213	0.024 / 0.069 / 0.095	0.044 / 0.060 / 0.079
	AutoIV	16.775 / 2.015 / 2.158	0.236 / 0.242 / 0.254	0.000 / 0.000 / 0.000	0.041 / 0.057 / 0.085
	VIV	18.499 / 7.769 / 4.560	0.032 / 0.065 / 0.115	0.037 / 0.052 / 0.099	0.037 / 0.068 / 0.072
	GIV	0.850 / 0.970 / 1.879	0.154 / 0.166 / 0.207	0.020 / 0.033 / 0.066	0.028 / 0.058 / 0.084
Linear No Candidate (no U)	TrueIV	—	—	—	—
	ZNet	115.223 / 2.995 / 2.728	0.147 / 0.156 / 0.190	0.031 / 0.062 / 0.082	— / — / —
	AutoIV	12.631 / 2.437 / 2.154	0.216 / 0.232 / 0.250	0.000 / 0.000 / 0.000	— / — / —
	VIV	21.595 / 5.473 / 4.768	0.031 / 0.054 / 0.116	0.037 / 0.047 / 0.113	— / — / —
	GIV	1.574 / 0.649 / 1.787	0.161 / 0.164 / 0.200	0.022 / 0.018 / 0.062	— / — / —

Table 12. Instrument Strength and Validity on Non-linear Synthetic Dataset.

Dataset	IV Method	F-Stat(Z,T) (Relevance) (Train/Val/Test)	Corr(Z,C) (Independence) (Train/Val/Test)	Corr(Z,Y-Yhat) (Exogeneity) (Train/Val/Test)	Corr(Z,U) (Independence) (Train/Val/Test)
Non-linear Disjoint	TrueIV	10.436 / 4.195 / 2.690	0.027 / 0.051 / 0.124	0.079 / 0.078 / 0.108	0.030 / 0.062 / 0.045
	ZNet	298.079 / 24.161 / 14.563	0.163 / 0.178 / 0.192	0.031 / 0.049 / 0.080	0.285 / 0.256 / 0.257
	AutoIV	102.265 / 24.380 / 18.903	0.206 / 0.217 / 0.227	0.000 / 0.000 / 0.000	0.278 / 0.241 / 0.295
	VIV	16.532 / 5.867 / 5.673	0.033 / 0.058 / 0.114	0.034 / 0.047 / 0.094	0.059 / 0.069 / 0.102
	GIV	17.338 / 5.966 / 5.895	0.141 / 0.150 / 0.181	0.036 / 0.048 / 0.074	0.144 / 0.140 / 0.176
Non-linear Disjoint (no $U \rightarrow X$)	TrueIV	19.393 / 6.986 / 5.568	0.027 / 0.051 / 0.124	0.028 / 0.055 / 0.115	0.030 / 0.044 / 0.094
	ZNet	70.675 / 7.622 / 4.336	0.143 / 0.157 / 0.174	0.017 / 0.053 / 0.105	0.033 / 0.046 / 0.081
	AutoIV	40.857 / 6.378 / 3.899	0.236 / 0.236 / 0.260	0.000 / 0.000 / 0.000	0.031 / 0.043 / 0.090
	VIV	17.436 / 5.063 / 4.857	0.034 / 0.056 / 0.117	0.042 / 0.051 / 0.101	0.034 / 0.058 / 0.076
	GIV	2.574 / 1.176 / 1.936	0.140 / 0.148 / 0.187	0.042 / 0.039 / 0.067	0.035 / 0.060 / 0.072
Non-linear Latent Categorical	TrueIV	96.409 / 39.441 / 8.684	0.204 / 0.212 / 0.235	0.009 / 0.011 / 0.025	0.064 / 0.083 / 0.022
	ZNet	120.953 / 20.441 / 7.507	0.173 / 0.172 / 0.188	0.030 / 0.069 / 0.099	0.174 / 0.178 / 0.179
	AutoIV	58.730 / 12.420 / 9.422	0.213 / 0.221 / 0.236	0.000 / 0.000 / 0.000	0.251 / 0.231 / 0.250
	VIV	15.337 / 3.719 / 4.762	0.034 / 0.061 / 0.113	0.034 / 0.043 / 0.091	0.037 / 0.063 / 0.083
	GIV	57.630 / 20.981 / 10.098	0.131 / 0.142 / 0.169	0.025 / 0.035 / 0.068	0.118 / 0.103 / 0.149
Non-linear Latent Categorical (no $U \rightarrow X$)	TrueIV	129.011 / 37.750 / 14.270	0.204 / 0.212 / 0.235	0.005 / 0.020 / 0.029	0.033 / 0.050 / 0.071
	ZNet	120.243 / 19.860 / 9.497	0.148 / 0.150 / 0.193	0.019 / 0.054 / 0.077	0.025 / 0.054 / 0.071
	AutoIV	79.648 / 20.792 / 7.362	0.253 / 0.267 / 0.273	0.000 / 0.000 / 0.000	0.032 / 0.049 / 0.091
	VIV	16.644 / 6.861 / 4.575	0.033 / 0.061 / 0.117	0.033 / 0.057 / 0.106	0.040 / 0.065 / 0.087
	GIV	34.207 / 11.849 / 5.966	0.141 / 0.146 / 0.169	0.017 / 0.039 / 0.058	0.028 / 0.057 / 0.087
Non-linear Mixed	TrueIV	4.313 / 1.787 / 2.142	0.027 / 0.051 / 0.124	0.058 / 0.098 / 0.102	0.030 / 0.062 / 0.045
	ZNet	144.440 / 18.633 / 15.304	0.167 / 0.156 / 0.189	0.036 / 0.083 / 0.107	0.201 / 0.185 / 0.221
	AutoIV	94.883 / 17.895 / 17.240	0.210 / 0.222 / 0.238	0.000 / 0.000 / 0.000	0.224 / 0.210 / 0.248
	VIV	15.459 / 4.695 / 3.970	0.035 / 0.058 / 0.111	0.043 / 0.068 / 0.117	0.052 / 0.062 / 0.091
	GIV	56.539 / 18.722 / 9.017	0.138 / 0.145 / 0.194	0.034 / 0.043 / 0.077	0.136 / 0.126 / 0.153
Non-linear Mixed (no $U \rightarrow X$)	TrueIV	16.903 / 4.576 / 3.954	0.027 / 0.051 / 0.124	0.026 / 0.057 / 0.120	0.027 / 0.055 / 0.085
	ZNet	281.071 / 28.446 / 19.673	0.236 / 0.239 / 0.275	0.020 / 0.038 / 0.071	0.043 / 0.059 / 0.067
	AutoIV	163.159 / 34.251 / 23.897	0.229 / 0.235 / 0.257	0.000 / 0.000 / 0.000	0.031 / 0.063 / 0.069
	VIV	19.235 / 3.738 / 4.668	0.035 / 0.059 / 0.114	0.034 / 0.065 / 0.099	0.032 / 0.064 / 0.087
	GIV	24.444 / 8.313 / 5.430	0.137 / 0.160 / 0.188	0.024 / 0.036 / 0.061	0.032 / 0.053 / 0.079
Non-linear No Candidate	TrueIV	—	—	—	—
	ZNet	54.003 / 9.565 / 4.068	0.144 / 0.186 / 0.187	0.022 / 0.061 / 0.091	0.198 / 0.195 / 0.191
	AutoIV	62.921 / 16.672 / 6.355	0.202 / 0.201 / 0.236	0.000 / 0.000 / 0.000	0.322 / 0.324 / 0.318
	VIV	20.382 / 4.410 / 4.932	0.034 / 0.057 / 0.115	0.031 / 0.047 / 0.096	0.040 / 0.060 / 0.090
	GIV	23.479 / 3.748 / 3.176	0.145 / 0.147 / 0.182	0.029 / 0.028 / 0.069	0.091 / 0.098 / 0.099
Non-linear No Candidate (no $U \rightarrow X$)	TrueIV	—	—	—	—
	ZNet	100.546 / 7.451 / 6.169	0.114 / 0.121 / 0.171	0.033 / 0.063 / 0.081	0.043 / 0.052 / 0.075
	AutoIV	55.722 / 7.239 / 7.235	0.215 / 0.217 / 0.246	0.000 / 0.000 / 0.000	0.033 / 0.054 / 0.073
	VIV	19.903 / 7.638 / 5.995	0.033 / 0.062 / 0.118	0.039 / 0.049 / 0.108	0.039 / 0.060 / 0.073
	GIV	71.468 / 20.206 / 8.957	0.151 / 0.153 / 0.190	0.021 / 0.036 / 0.066	0.041 / 0.058 / 0.086
Non-linear No Candidate (no U)	TrueIV	—	—	—	—
	ZNet	97.217 / 3.587 / 3.745	0.144 / 0.149 / 0.207	0.032 / 0.039 / 0.110	— / — / —
	AutoIV	40.972 / 4.580 / 5.317	0.215 / 0.222 / 0.251	0.000 / 0.000 / 0.000	— / — / —
	VIV	18.745 / 3.922 / 5.198	0.031 / 0.063 / 0.109	0.022 / 0.063 / 0.118	— / — / —
	GIV	87.656 / 21.257 / 17.612	0.145 / 0.151 / 0.184	0.031 / 0.036 / 0.080	— / — / —

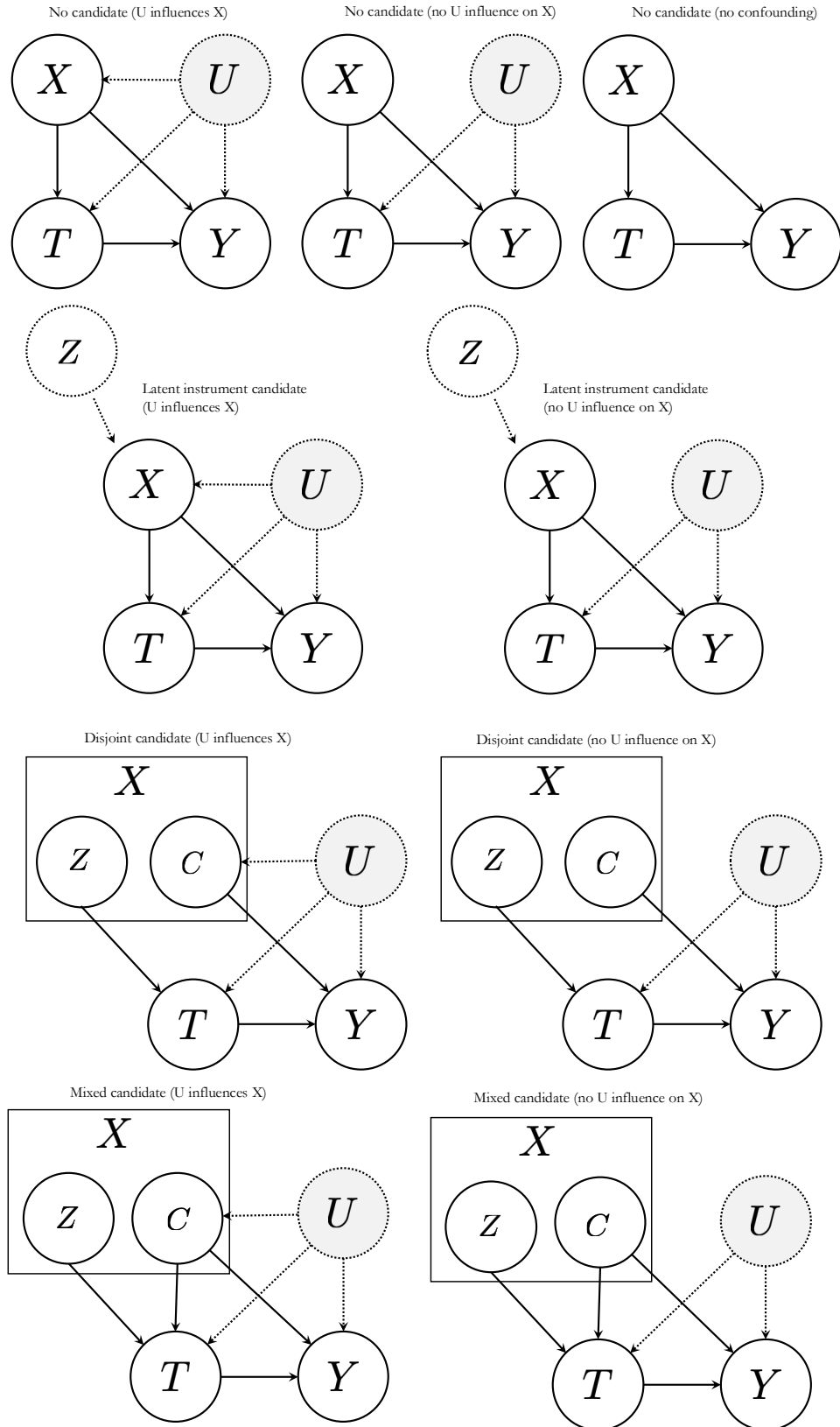


Figure 7. Directed acyclic graphs (DAGs) demonstrating the various data generation processes on which ZNet is evaluated. Linear and non-linear relationships are constructed for each DAG giving 18 total datasets for evaluation. Maintext results focus on cases where U influences X as this is more challenging, more general, and unique to ZNet.